2008-03-31

Compact Waveguide Splitter Networks

Seunghyun Kim

Gregory P. Nordin
nordin@byu.edu

Weisheng Hu

Yusheng Qian

Jiguo Song

Original Publication Citation

Y. Qian, J. Song, S. Kim, W. Hu, G. P. Nordin, "Compact waveguide splitter networks," Optics Express 16(7), pp. 4981-499 (28). http://www.opticsexpress.org/abstract.cfm?id=156939.

Compact waveguide splitter networks

Yusheng Qian, Jiguo Song, Seunghyun Kim, Weisheng Hu, and Gregory P. Nordin

Electrical and Computer Engineering, Brigham Young University,Provo, UT 84602 USA
nordin@ee.byu.edu

Abstract: We demonstrate compact waveguide splitter networks in silicon-on-insulator (SOI) rib waveguides using trench-based splitters (TBSs) and bends (TBBs). Rather than a 90° geometry, we use 105° TBSs to facilitate reliable fabrication of high aspect ratio trenches suitable for 50/50 splitting when filled with SU8. Three dimensional (3D) finite difference time domain (FDTD) simulation is used for splitter and bend design. Measured TBB and TBS optical efficiencies are 84% and 68%, respectively. Compact 105° 1 × 4, 1 × 8, and 1 × 32 trench-based splitter networks (TBSNs) are demonstrated. The measured total optical loss of the 1 × 32 TBSN is 9.15 dB. Its size is only 700 μm × 1600 μm for an output waveguide spacing of 50 μm.

OCIS codes: (130.0130) Integrated optics; (230.1360) Beam splitters; (260.6970) Total internal reflection; (230.7370) Waveguides; (130.1750) Components; (250.5300) Photonic integrated circuits.

References and Links

1. J. Gamet and G. Pandraud, "Field-matching Y-branch for low loss power splitter," Opt. Commun. **248**, 423-429 (2005).
2. Y. Sakamaki, T. Saida, M. Tamura, T. Hashimoto, and H. Takahashi, "Low-loss Y-branch waveguides designed by wavefront matching method and their application to a compact 1 × 32 splitter," Electron. Lett. **43**, 217-219 (2007).
3. K. B. Mogensen, Y. C. Kwok, J. C. T. Eijkel, N. J. Peterson, A. Manz, and J. P. Kutter, "A microfluidic device with an integrated waveguide beam splitter for velocity measurements of flowing particles by Fourier transformation," Anal. Chem. **75**, 4931-4936 (2003).
4. A. Cleary, S. Garcia-Blanco, A. Glidle, J. S. Aitchison, P. Laybourn, and J. M. Cooper, "An integrated fluorescence array as a platform for lab-on-a-chip technology using multimode interference splitters," IEEE Sens. J. **5**, 1315-1320 (2005).
5. Y. Hibino, F. Hanawa, H.Nakagome, M. Ishii, and N. Takato, Member, IEEE, "High reliability optical splitters composed of silica-based planar lightwave circuits," J. Lightwave Technol. **13**, 1728-1735 (1995).
6. Y. Hida and Y. Inoue, Member, IEEE, F. Hanawa, T. Fukumitsu, Y. Enomoto, and N. Takato, Member, IEEE, "Silica-based 1×32 splitter integrated with 32 WDM couplersusing multilayered dielectric filters for fiber line testing at 1.65μm," IEEE Photon. Technol. Lett. **11**, 96-98 (1999).
7. M. Bouda, J. W. M. van Uffelen, C. van Dam, and B. H. Verbeek, "Compact 1×16 power splitter based on symmetrical 1×2MMI splitters," Electron. Lett. **21**, 1756-1758 (1994).
8. B. Jalali, S. Yegnanarayanan, T. Yoon, T. Yoshimoto, I. Rendina, and F. Coppinger, "Advances in Silicon-on-Insulator Optoelectronics," IEEE J. Sel. Top. Quantum Electron. **4**, 938-947 (1998).
9. J. H. Kim, B. W. Dudley, and P. J. Moyer, "Experimental demonstration of replicated multimode interferometer power splitter in Zr-doped sol-gel," J. Lightwave Technol. **24**, 612-616 (2006).
10. Y. Qian, J. Song, S. Kim, and G. P. Nordin, "Compact 90° trench-based splitter for silicon-on-insulator rib waveguides," Opt. Express **15**, 16712-16718 (2007).
11. N. Rahmanian, S. Kim, Y. Lin, G. P. Nordin, "Air-trench splitters for ultra-compact ring resonators in low refractive index contrast waveguides," Opt. Express **16**, 456-465 (2008).
12. Y. Qian, S. Kim, J. Song, and G. P. Nordin, "Compact and low loss silicon-on-insulator rib waveguide 90° bend," Opt. Express **14**, 6020-6028 (2006).
13. G. P. Nordin, J. W. Noh, and S. Kim, "In-plane photonic transduction for microcantilever sensor arrays," SPIE **6447**, 64470J (2007).
14. J. Fritz, M. K. Baller, H. P. Lang, H. Rothuizen, P. Vettiger, E. Meyer, H. J. Guntherodt, Ch. Gerber, and J.K. Gimzewski, "Translating biomolecular recognition into nanomechanics," Science **288,** 316-318 (2000).
15. G. Wu, R. H. Datar, K. M. Hansen, T. Thundat, R. J. Cote, and A. Majumdar, "Bioassay of prostate-specific antigen (PSA) using microcantilevers," Nat. Biotechnol **19,** 856-860 (2001).

#92636 - $15.00 USD Received 11 Feb 2008; revised 23 Mar 2008; accepted 25 Mar 2008; published 27 Mar 2008

16. F. Huber, M. Hegner, C. Gerber, H. J. Guntherodt, and H. P. Lang, "Label free analysis of transcription factors using microcantilever arrays," Biosens. Bioelectron **21,** 1599-1605 (2006).
17. A. Taflove, *Computational Electrodynamics: The Finite-Difference Time-Domain Method*, (Artech House, Boston, Mass., 1995).
18. J. Cai, G. P. Nordin, S. Kim, and J. Jiang, "Three-dimensional analysis of a hybrid photonic crystal-conventional waveguide 90° bend," Appl. Opt. **43**, 4244-4249 (2004).
19. J. P. Berenger, "A perfectly matched layer for the absorption of electromagnetic waves," J. Comput. Phys. **114**, 185-200 (1994).

1. Introduction

Waveguide splitter networks that divide an optical signal into N outputs (1 × N) are important elements in a variety of applications including power splitters for planar lightwave circuits (PLCs) [1,2] and periodic optical sources for integrated microfluidic devices [3,4]. Such splitter networks are primarily based on either cascaded Y-branch splitters [1-3,5,6] or multimode interference (MMI) splitters [4,7-9]. In this paper we report an alternate approach using trench-based splitters (TBSs) [10,11] and trench-based bends (TBBs) [12]. We focus on silicon-on-insulator (SOI) rib waveguides that have low in-plane core/clad refractive index contrast and hence require relatively large bend radius (1.2 mm for the waveguides considered in this paper) which limits achievable size reduction for traditional splitter networks. The use of TBSs and TBBs to create trench-based splitter networks (TBSNs) results in a large decrease in required chip area. This is particularly important in our ultimate application of sourcing light into many SOI microcantilevers for a new in-plane photonic transduction mechanism [13] to enable single-chip microcantilever sensor arrays [14-16].

In this paper we first discuss modification of our previously-reported SOI TBSs [10] to achieve 50/50 reflection/transmission splitting ratios in fabricated splitters with SU8 as the trench fill material by changing the splitter angle from 90° to 105°. We then report fabrication and measurement of 105° 1 × 4 and 1 × 32 TBSNs, followed by an examination of total splitter network loss. For an output waveguide spacing of 50 μm, the 1 × 32 network occupies an area of only 700 μm × 1600 μm.

2. Design

As shown in Fig. 1(a), we consider an SOI rib waveguide with rib width of 1.6 μm, rib thickness of 0.75 μm, and slab thickness of 0.65 μm. The underclad is SiO_2 and the overclad is SU8, which is the same material used to fill the TBS and TBB trenches. The waveguide supports only the fundamental TE polarization mode (electric field in the plane of the silicon) at a wavelength of 1550 nm.

Figures 1(b) and 1(c) show the geometry of a TBB and a TBS. The TBB bend angle, α_1, is defined as the angle between the original waveguide direction and the direction of the output waveguide. Similarly, the TBS bend angle, α_2, is defined as the angle between the transmission output direction and the reflection output direction. In both cases, D is defined as the distance from the intersection of the waveguide center lines to the first interface of the trench. In Ref. 12 we reported fabrication and measurement of TBBs with a 90° bend angle in which the trench is filled with SU8 and the measured optical efficiency (i.e. fraction of the incident waveguide mode power reflected into the mode of the output waveguide) is 93%. In Ref. 10 we reported the development of SOI TBSs with a 90° bend angle. TBSs filled with air (n = 1.0), SU8 (n = 1.57), or refractive index matching fluid (n = 1.733) are characterized at 1550 nm. A 49/51 (reflection/transmission) splitting ratio is reported for a trench width of 82 nm with index matching fluid as the trench fill material. However, TBSs with SU8 as the trench fill material need a trench width of 67 nm to achieve a 50/50 splitting ratio, which is too small for us to reliably fabricate since the trench etch depth must be 750 nm. To realize 50/50 TBSs with SU8 as the trench fill material, in this paper we explore a new design by

#92636 - $15.00 USD Received 11 Feb 2008; revised 23 Mar 2008; accepted 25 Mar 2008; published 27 Mar 2008

increasing the TBS bend angle to 105° so that a 50/50 splitting ratio can be achieved with a wider trench.

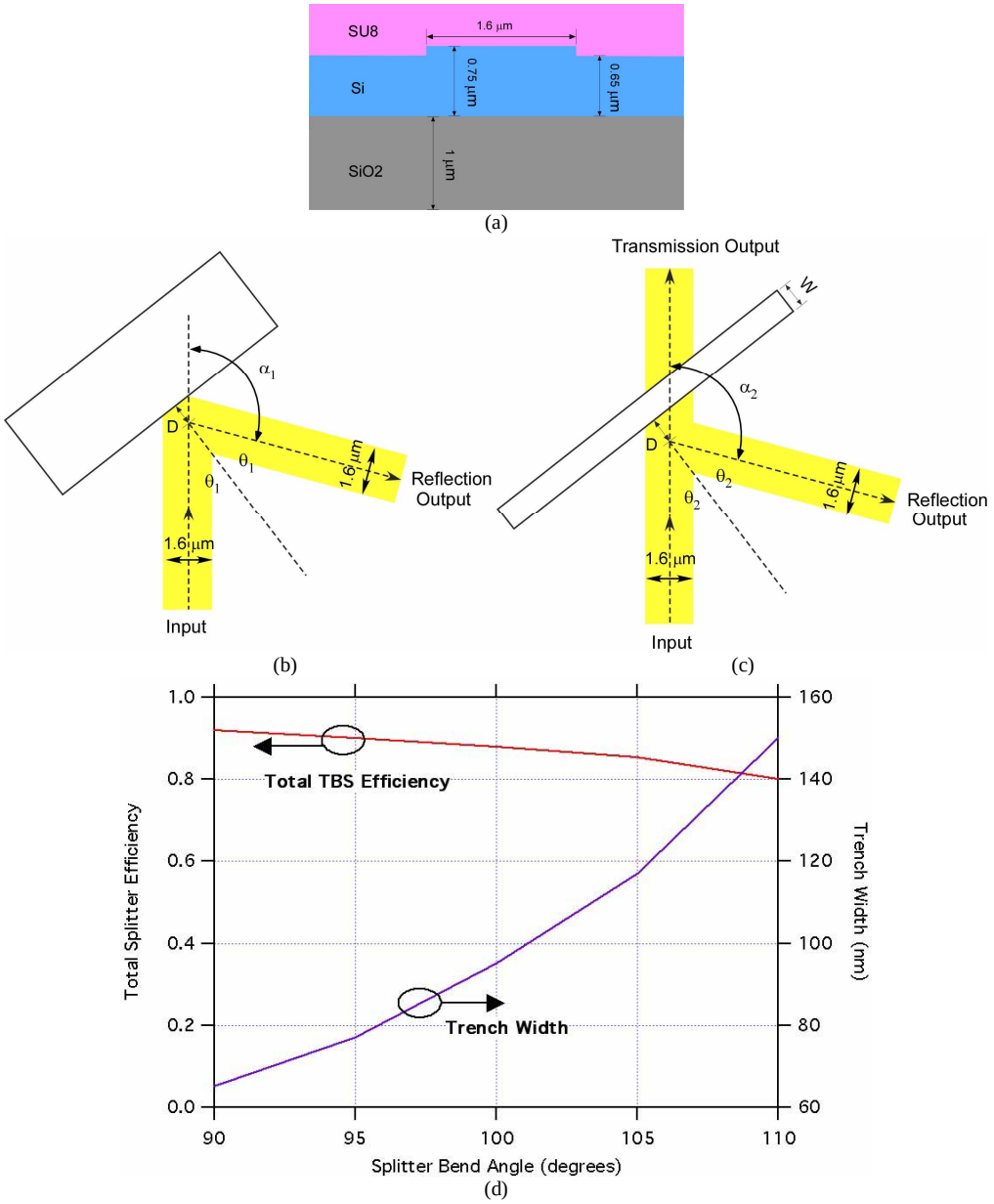

Fig. 1. (a). Rib waveguide cross section. (b) 105° TBB and (c) TBS geometry (i.e., $\alpha_1 = \alpha_2 = 105°$ and $\theta_1 = \theta_2 = 37.5°$). (d) Required trench width for 50/50 splitting using SU8 filled TBSs (right axis) and total splitter efficiency (left axis) as a function of splitter bend angle.

As discussed in Ref. [10], TBSs operate based on frustrated total internal reflection (FTIR) in which the trench width is small enough that part of the optical field is transmitted through the trench while the rest undergoes total internal reflection. For a given incidence angle,

$$\theta_2 = 90° - \alpha_2/2, \tag{1}$$

#92636 - $15.00 USD Received 11 Feb 2008; revised 23 Mar 2008; accepted 25 Mar 2008; published 27 Mar 2008

the ratio between the reflected and transmitted power is a function of trench width. Alternatively, for a given trench width, the splitting ratio can be altered by changing the incidence angle (i.e., splitter bend angle). We use the three dimensional (3D) finite difference time domain (FDTD) method [17,18] with Berenger PML boundary conditions [19] to explore the relationship between trench width and splitter angle to achieve 50/50 splitting for the case of SU8 trench fill, which is also the overclad material of the SOI rib waveguide. The refractive indices used for numerical simulation are 3.476 for silicon, 1.444 for SiO_2, and 1.570 for SU8 at a wavelength of 1550 nm. The result is shown in Fig. 1(d) in which the trench width (right axis) is shown as a function of splitter bend angle for 50/50 splitting. Also shown is the total optical efficiency (i.e., sum of transmitted and reflected mode power divided by incident mode power) on the left axis. Note that as the splitter bend angle increases the required trench width also increases, but the total optical efficiency is reduced. Based on fabrication considerations, we choose a splitter bend angle of 105° such that the desired trench width is 116 nm while the total optical efficiency is 84% (reflection 42% and transmission 42%). To account for the Goos-Hanchen shift, D is chosen to be -97 nm. The TBS trench has an aspect ratio (depth:width) of 6.5:1, which is relatively straightforward for us to fabricate. A plot of the magnitude of the time-averaged magnetic field is shown at a plane 0.325 μm above the SiO_2 underclad (i.e., nearly in the middle of the rib waveguide) in Fig. 2(a).

Changing the splitter bend angle, α_2, to 105° necessitates changing α_1 for the TBBs to 105° to maintain the desired geometry of the TBSNs (shown in later sections). We similarly use 3D FDTD to design the 105° bends. Figure 2(b) shows the magnitude of the time-averaged magnetic field in a plane 0.325 μm above the SiO_2 underclad for a 105° SU8 filled TBB (D = -85 nm), which has an optical efficiency of 82%.

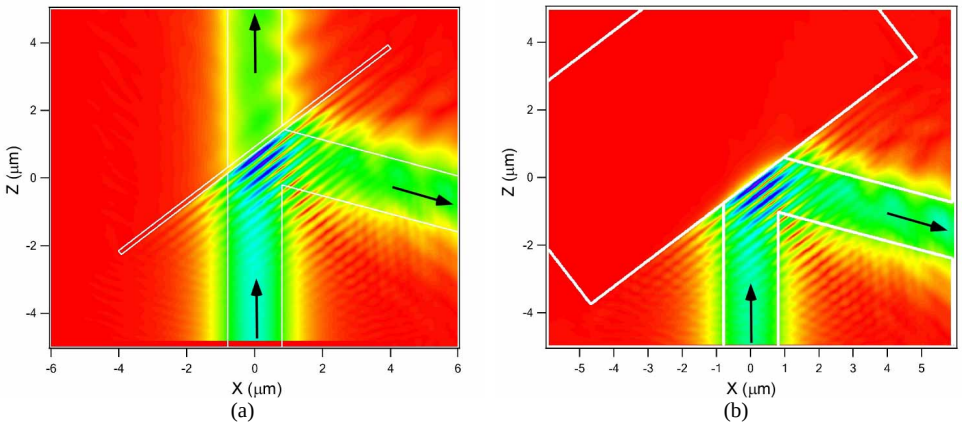

Fig. 2. Magnitude of the time-averaged magnetic field for (a) 105° TBS and (b) 105° TBB.

3. Measured 105° TBB and TBS optical properties

The 105° TBBs and TBSs are fabricated with the same process as the 90° geometry devices reported in Refs. [10] and [12]. Electron beam lithography (EBL) with a Nanometer Pattern Generation System (JC Nabity NPGS) and field emission environmental scanning electron microscope (FEI/Philips XL30 ESEM-FEG) is used for trench patterning. A water soluble conductive polymer (aquaSAVE53za) is spin coated on top of the electron-beam resist (ZEP 520A) to prevent charging during EBL. After developing, trenches are etched in an inductively coupled plasma reactive ion etcher (ICP RIE) with a fluorine-based etch chemistry. Finally, SU8 is spin coated to fill the trenches and also act as the upper cladding.

#92636 - $15.00 USD Received 11 Feb 2008; revised 23 Mar 2008; accepted 25 Mar 2008; published 27 Mar 2008

The optical source for characterization of TBBs and TBSs is an amplified spontaneous emission (ASE) source with a center wavelength of 1550 nm connected to an erbium-doped fiber amplifier (EDFA). A non-laser source source is chosen because the ASE bandwidth (~30 nm) results in a short coherence length which eliminates Fabry-Perot effects in the waveguides that would otherwise be present because of light reflected from the chip output and input endfaces. Note that the bandwidth of the source does not significantly affect our measurement results because the bend and splitter performance are only weakly dependent on wavelength. Light from the EDFA passes through a linear polarizer and is coupled into a polarization maintaining (PM) fiber, which in turn is butt coupled to an input waveguide on the chip under test. A single mode fiber is butt coupled to an output waveguide to direct light to a detector. A Newport auto-align system is used to maximize the coupling through the input and output fibers [10,12].

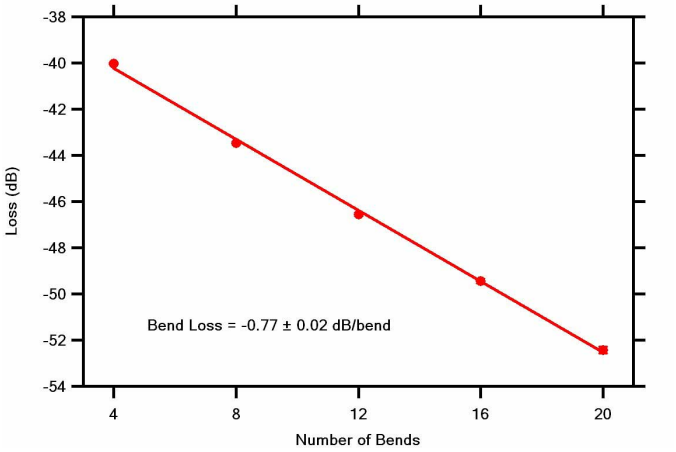

Fig. 3. Measured loss of 105° TBB as a function of number of bends in a set of equal-length waveguides. The average error for each data point is +/-0.09 dB. The insertion loss is ~37 dB, with almost all of this (~36 dB) due to the fiber/waveguide mode mismatch in getting light on and off chip.

The optical properties of the 105° TBBs and TBSs are characterized as discussed in Refs. 10 and 12 for 90° devices. The optical loss for 105° TBBs is measured with a set of equal length waveguides that have different numbers of bends. Figure 3 shows the measured optical loss as a function of the number of bends. The measured loss of 105° TBBs is -0.77 dB ± 0.02 dB (84%) per bend. Curiously, the measured efficiency is slightly higher than the 3D FDTD prediction of 82%. However, this is consistent with our experience for 90° TBBs in which the measured efficiency is 93% while the 3D FDTD prediction is 89%. We have not yet discovered the source of this discrepancy.

For TBSs, the splitter ratio and efficiency is measured using sets of 105° 1 × 2 network structures that contain one TBS and one TBB. Figure 4(a) shows a fabricated 105° 1 × 2 network before coating SU8. The two etched circular regions at each end of the splitter trench are intended to facilitate filling SU8 into the trench. The other etched circles are present to scatter stray light in the silicon slab which originates from butt coupling the input fiber to the input waveguide. Measurement results for the reflection and transmission splitting ratio (i.e., reflected or transmitted optical power divided by the sum of the two) for individual splitters with different trench widths are shown in Fig. 4(b). Also shown are 3D FDTD simulation results. The short dashed lines are linear fits to the measured data. While the slope of these lines is comparable to the 3D FDTD results near the 50/50 splitting ratio region, the actual trench width at which 50/50 splitting occurs is 95 nm for the measured data compared to 116

#92636 - $15.00 USD Received 11 Feb 2008; revised 23 Mar 2008; accepted 25 Mar 2008; published 27 Mar 2008

nm for the simulations. The reason for this discrepancy is the fabricated trench widths are measured nondestructively by scanning electron microscope (SEM) imaging of the top of the trenches (i.e., looking down on the trenches from above the plane of the silicon). However, when an etched trench is cleaved and imaged in cross section as shown in Fig. 4(c), the trench sidewalls are seen to exhibit bowing. The center of the trench is 25% wider than the top trench width and therefore the effective trench width as experienced by the waveguide mode is larger than predicted by top-view SEM imaging.

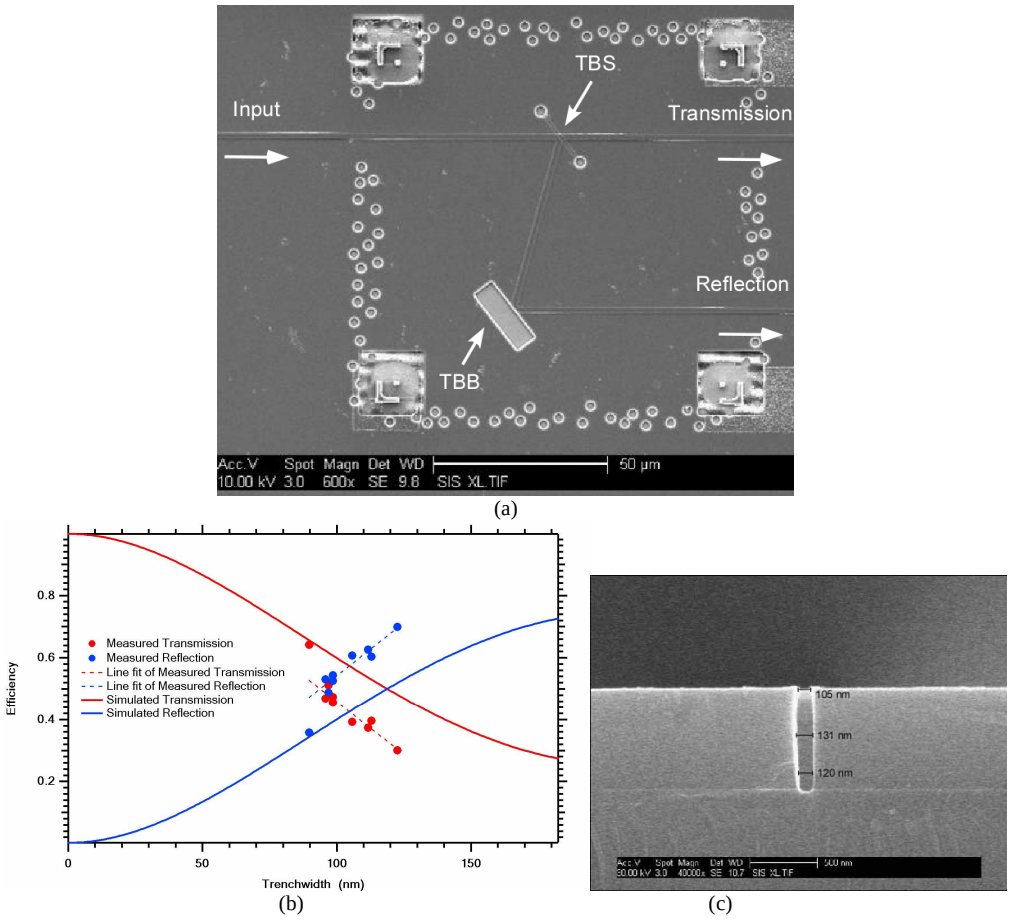

Fig. 4. (a). SEM image of a fabricated 1 × 2 network before SU8 spin coating. The separation between transmission and reflection waveguides is 50 µm. (b) Measurement and 3D FDTD simulation results for 105° TBS splitting ratio as a function of trench width. (c) Cross sectional SEM image of a cleaved trench.

The optical efficiency, η_{TBS}, of 105° TBSs can be experimentally determined based on [10]

$$\eta_{TBS} = \frac{P_{TBS\_reflection}/\eta_{TBB} + P_{TBS\_transmission}}{P_{Straight\_waveguide}} \tag{2}$$

where η_{TBB} is the optical efficiency of a 105° TBB, $P_{TBS\_reflection}$ and $P_{TBS\_transmission}$ are the measured TBS reflected and transmitted power, respectively, and $P_{Straight\_waveguide}$ is the measured power through a separate straight waveguide. The measured splitter efficiency

#92636 - $15.00 USD Received 11 Feb 2008; revised 23 Mar 2008; accepted 25 Mar 2008; published 27 Mar 2008

based on Eq. (2) is 67.8% ± 9.9% (-1.79 dB ± 0.66 dB). Increasing the verticality of etched trench sidewalls to remove the observed bowing should significantly improve TBS efficiency.

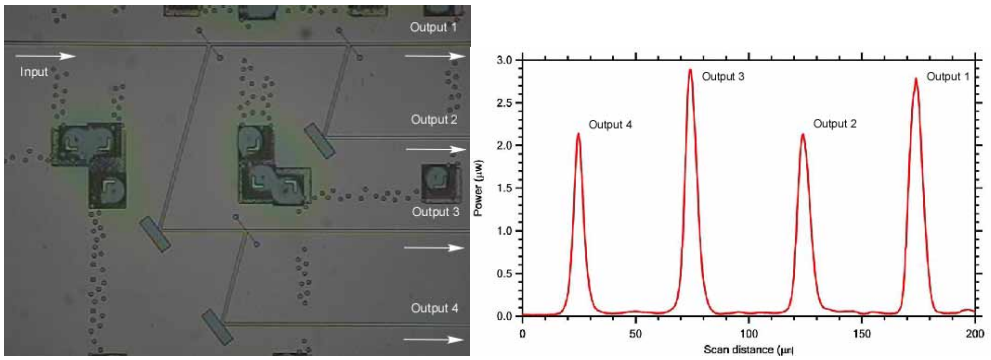

(a) (b)

Fig. 5. (a). Microscope image and (b) 1D output fiber scan of SU8 coated 1 × 4 105° TBSN.

4. 1 × N 105° TBSN Measurements

With 105° TBBs and TBSs successfully demonstrated, we combine them to make 1 × N networks. We use 1 cm × 1 cm die designed such that we can fabricate 1 × 4, 1 × 8, or 1 × 32 105° TBSNs. The TBSs of the network are fabricated to have a top-view trench width of ~95 nm to account for sidewall bowing. Figure 5(a) shows a microscope picture of a fabricated 1 × 4 network with 50 μm output waveguide spacing with SU8 on top. Figure 5(b) shows the measured optical power as a fiber is scanned along the output waveguides. The measured optical power through a straight waveguide is 23.7 μW so the optical efficiencies for outputs 1-4 are 12%, 9%, 12%, and 9%, respectively.

Figure 6(a) shows a 1 × 32 TBSN. The output waveguide spacing is 50 μm except for outputs #16 and #17 which have a spacing of 100 μm. The total 1 × 32 network region occupies an area only 700 μm × 1600 μm. Figure 6(b) is an infrared camera image of the 32 corresponding outputs. The optical power of each output is measured and plotted in Fig. 6(c). The 1×32 network has an average output power of 0.12 μw and a standard deviation (STD) of 0.03 μw. The normalized STD (STD divided by the mean) of the measured 32 outputs is 0.26. The optical power through a nearby straight waveguide is 32.8 μW so the average fraction of the input light that exits a given output waveguide is 0.37%.

Due to the asymmetry of our TBSN structure, light in different output waveguides passes through different numbers of TBBs. Consequently, there will be variation in the output optical powers due to losses from the TBBs. To estimate the expected variation for an ideal TBSN, we calculate the normalized output power of a 1 × 32 TBSN using the measured 105° TBB and TBS efficiency reported in Section 3, and assume that all of the TBSs in the network have a 50/50 splitting ratio (i.e., TBB efficiency 84% and TBS transmission and reflection efficiencies both 34%). The result is a normalized STD of 0.20. Comparing with the normalized STD of the measured 32 output powers (0.26), the variation of output power in the fabricated 1 × 32 network is ~30% higher than the theoretical value, which is most likely due to variations between individual splitters because of fabrication process nonuniformities and variations introduced by the quality of the endface polish. We note that TBSN output uniformity can be improved by using a symmetric 105° network geometry in which the number of TBBs in each output path is the same. However, the achieved level of uniformity reported in this paper is entirely adequate for our application since differential signals are used to transduce microcantilever deflection [13].

As a final comment on output uniformity, light exiting each output waveguide goes through a different waveguide propagation length. For our 1 × 32 network, the longest path

#92636 - $15.00 USD Received 11 Feb 2008; revised 23 Mar 2008; accepted 25 Mar 2008; published 27 Mar 2008

(output waveguide #32) is 2 mm longer than the shortest one (#1). Since the measured propagation loss is 1.1 dB (measured with the cut-back method using a straight waveguide sample at 1550 nm), this length difference causes an extra loss of only 0.22 dB. Hence the network output power variation due to waveguide length difference is negligible compared to the variation caused by the different number of TBBs in each output path.

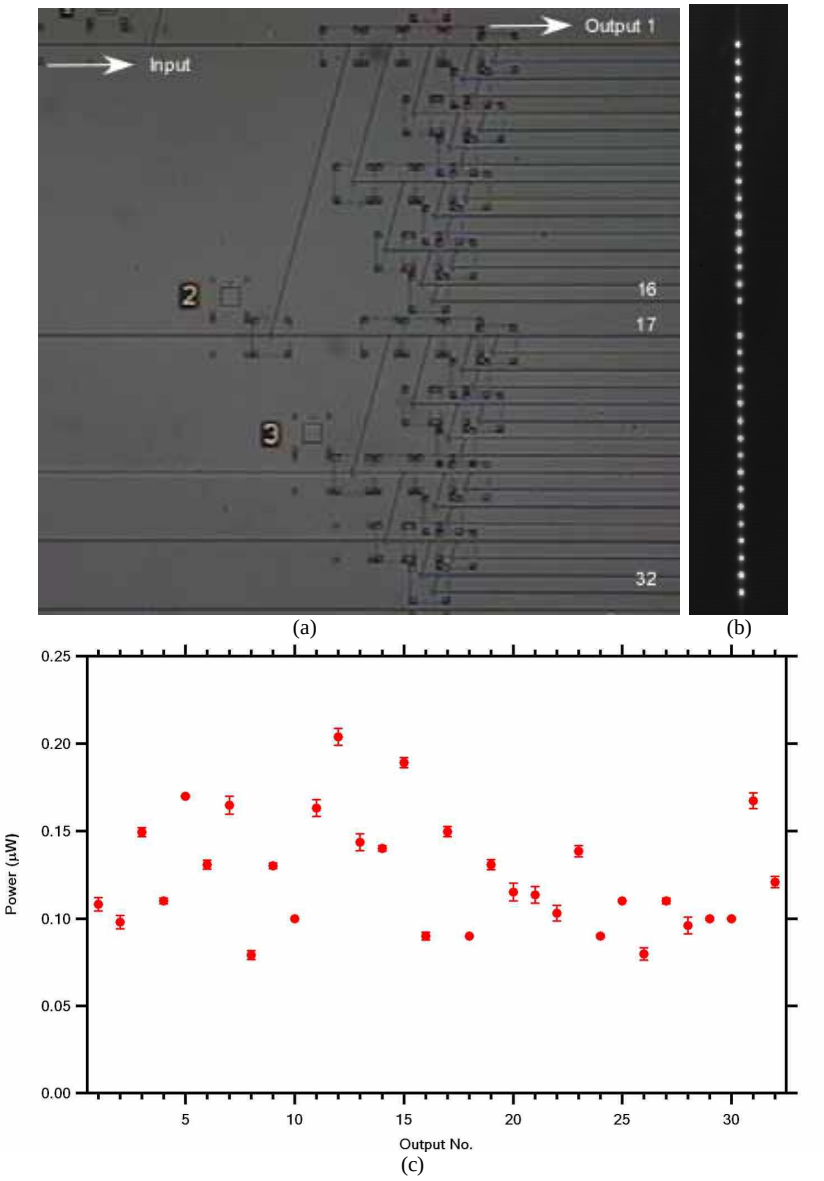

Fig. 6. (a). Microscope image of SU8 coated 1 × 32 TBSN and corresponding (b) IR camera image of output waveguides and (c) fiber-based output waveguide power measurement as a function of output waveguide number.

#92636 - $15.00 USD Received 11 Feb 2008; revised 23 Mar 2008; accepted 25 Mar 2008; published 27 Mar 2008

5. 1 × N 105° TBBSN loss

An important parameter to evaluate 1 × N network performance is the total optical loss of the network. We analyze this loss by assuming an ideal case in which the TBBs and TBSs of the network have same optical efficiency, η, and the TBS splitting ratio is 50/50. The total optical efficiency of a 1 × 2 network is the sum of the efficiency for the reflection path, $\eta^2/2$, and the efficiency for the transmission path, $\eta/2$. The total network loss can therefore be calculated as

$$L_{calc} = 10 * \log((\frac{\eta^2}{2} + \frac{\eta}{2})^M) \quad (3)$$

where M is the number of layers in the network, which is defined as the number of splitters that each waveguide passes from input to output. The output number N and the layer number M are related by $N = 2^M$.

The experimentally measured total network loss is

$$L_{meas} = 10 * \log(\frac{P_{1 \times \mathrm{N}\ network}}{P_{straight-waveguide}}) \quad (4)$$

where the network total output power, $P_{1 \times \mathrm{N}\ network}$, is the sum of all N output powers.

L_{calc} is plotted as a function of N and M (top and bottom axes, respectively) in Fig. 7 for η= 60%, 70%, 80%, 90%, and 95%. The measured total network loss, L_{meas}, is also shown (-3.82 dB, -5.9 dB, and -9.15 dB for 1 × 4, 1 × 8, and 1 × 32 TBSNs, respectively). In the case of the 1×8 network, the total output power is an estimated value based on only seven outputs (multiplying the average power of the seven outputs by eight) because one output waveguide of the network has a waveguide defect such that no output power can be measured. Note that the measured data indicates an average TBB/TBS efficiency between 70% and 80%, and that the data points are consistent with each other (i.e., nearly linear).

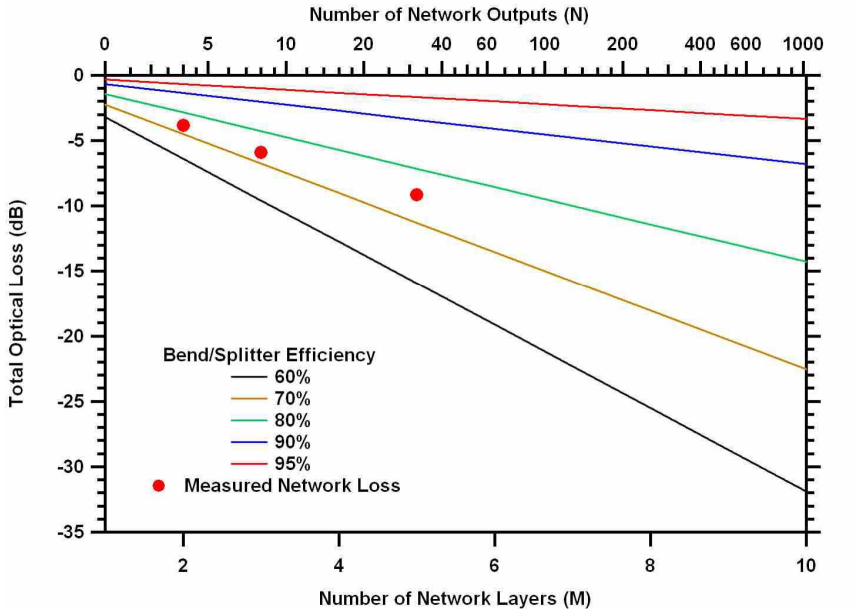

Fig. 7. Measured and calculated 1 × N network total loss as a function of number of network layers (bottom axis) and network outputs (top axis) (see text for details).

#92636 - $15.00 USD Received 11 Feb 2008; revised 23 Mar 2008; accepted 25 Mar 2008; published 27 Mar 2008

6. Conclusions

In summary, we have demonstrated 105° TBBs and TBSs with SU8 as the trench fill material. The measured optical efficiencies are 84% and 68% respectively. With a 105° splitter bend angle we are able to achieve 50/50 splitting for reasonable trench widths at the cost of somewhat lower total efficiency. Based on these 105° components, we have fabricated 1 × N networks up to 1 × 32, which occupies an area of only 700 μm × 1600 μm for output waveguide spacing of 50 μm. The total network loss for the 1 × 32 network is 9.15 dB, which is consistent with the measured TBB and TBS efficiencies. The normalized standard deviation of the output power in the network's 32 outputs is 0.26, which is only ~30% higher than what is expected based only on the asymmetry of the network.

Acknowledgment

This work was supported in part by NSF grants IIS-0641973 and ECS-0602261, and DARPA grant N66001-04-8933.

#92636 - $15.00 USD Received 11 Feb 2008; revised 23 Mar 2008; accepted 25 Mar 2008; published 27 Mar 2008